Appl Biochem Biotechnol (2009) 159:295–298
DOI 10.1007/s12010-007-8121-z

2D Polarization Imaging of Turbid Media

Nidhi Mathur · Naresh K. Chaudhary · Purnima Bharti

Received: 1 August 2007 / Accepted: 12 October 2007 /
Published online: 31 January 2008

Abstract Cancer normally tends to result in the decrease of tissue elasticity; i.e., the cancerous region is more rigid than the normal surrounding areas. This would appear as differences in the distribution of internal birefringence that could be used to improve image contrast between the cancerous and normal tissue structures. Different filtering techniques are used to enhance the image to help us identify, locate, and diagnose an "object," such as a tumor inside a biological tissue.

Keywords Mueller matrix · Imaging · Polarization · Turbid media

Introduction

One important property of light is its polarization (i.e., its direction in which the electric field points with respect to the direction of propagation of light). The propagation of polarized light through a biological tissue causes the polarization status of the photons to change because of tissue birefringence and scattering [1]. Imaging with polarized light can select light that backscatters from the superficial tissues, in contrast to the light that reflects from the air/tissue surface or light that propagates deep into the tissue before it eventually escapes as diffuse reflectance and whose polarization state has been fully randomized. Hence, images can characterize the superficial region of a tissue, which is often the region where cancer develops.

More than 85% of all cancers are epithelial in origin. Most epithelial cancers have a well-defined precancerous stage characterized by nuclear atypia and dysplasia [2]. Lesions

N. Mathur (✉)
Amity University, Lucknow, Uttar Pradesh, India
e-mail: mathurnidhi@rediffmail.com

N. K. Chaudhary
Dr. R.M.L. Avadh University, Faizabad, India

P. Bharti
University of Lucknow, Lucknow, Uttar Pradesh, India

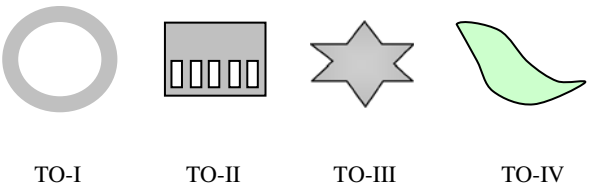

Fig. 1 Objects of various shapes immersed in the phantom

detected at this stage can potentially be eradicated with early diagnosis. However, many forms of atypia and dysplasia are not visually observable. Thus, surveillance for invisible dysplasia employs random biopsy, followed by microscopic examination of the biopsy material by a pathologist. Usually, only a small fraction of the epithelial surface at risk for dysplasia can be sampled in this way, potentially resulting in a high sampling error.

Polarization-based imaging measurements can provide an enhancement in superficial structures to allow for subsurface imaging [3, 4]. Tumor can be considered as an invisible, rigid object of different refractive index in a turbid media. Polarization properties of turbid media and the Mueller matrix imaging technique can be used to detect this tumor. Images thus obtained are processed further to enhance the visualization. Different filtering schemes are implemented with the help of the Matlab program to obtain better results.

Materials and Method

For experimental purposes, we prepared a tissue phantom TP-A (concentration—0.08%) by diluting 10% intralipid solution with distilled water. Intralipid is a polydisperse media-like tissue. However, it consists of spherical scatterers of mean diameter of 97±3 nm (distribution of diameter from 25 to 675 nm). Phantom was placed in a glass cuvette with internal dimensions 5×5cm×1 cm.

Objects of different shapes (Fig. 1), sizes (1–3 mm), and refractive indices (1.4–1.5) were immersed in the phantom one by one. All the objects were suspended in the phantom with the help of a thin wire (diameter 0.5 mm). These objects mimic rigid, invisible tumor in a phantom. Objects were placed at the distance of 0.5 cm away from the front surface of the cuvette (i.e., the surface being imaged by the CCD camera). Samples were named as TO-I, TO-II, TO-III, TO-IV, and TO-V.

Mueller matrix images [5] for each sample was obtained with the help of the experimental setup shown in Fig. 2. Initially, 49 images were taken with 49 different input/output combinations of polarizer/analyzer and retarder. These 49 images were then manipulated [6–7] to obtain the final 16-image Mueller Matrix.

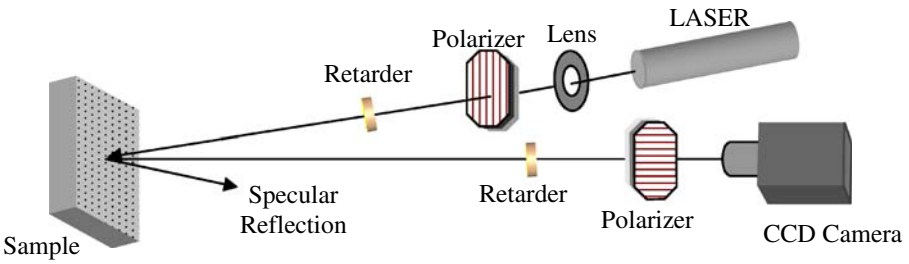

Fig. 2 Block diagram of the Mueller Matrix Polarization imaging system

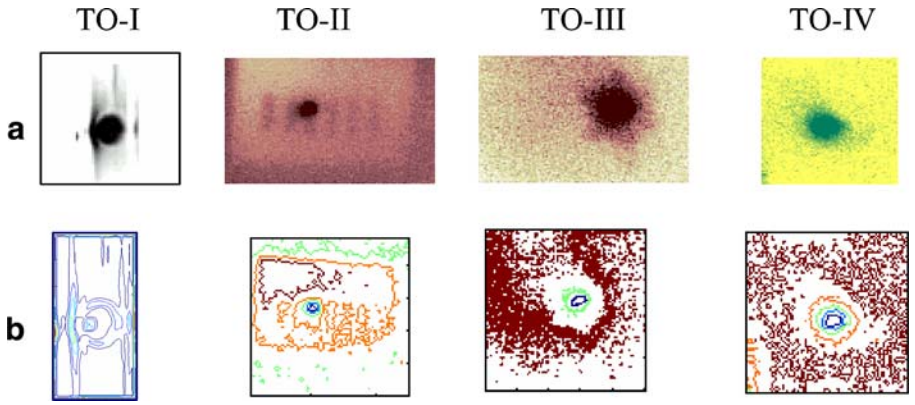

Fig. 3 (**a**) Images and (**b**) contours of M34 element of the Mueller matrix of the samples

Results and Discussion

M_{34} elements of the Mueller matrix images of the five samples are shown in Fig. 3a. Contours of the M_{34} element are shown in Fig. 3b. All these contours give a clear idea of the shape of the object immersed in the phantom. This strengthens our belief that the lesion governs the variation in the basic shapes of the contour in the matrices.

Through the application of appropriate filters the visualization can be improved. We took two samples together at a time for comparative study, TP-A (phantom without any object) and TO-I (phantom with ring). The final Mueller matrices obtained after computer processing are rearranged and the same matrix element of the two samples is placed side by side. The left side image is of the element of sample TP-A and the right one is of sample TO-I (Fig. 4).

Laplacian of Gaussian (*log*) filtering technique was applied on the images. There is a marked difference in the images of both the samples. Filtered image of sample TO-I clearly shows the presence of the wire and the ring. Similarly, after performing histogram equivalence operation, a bright ring is clearly visible in the sample.

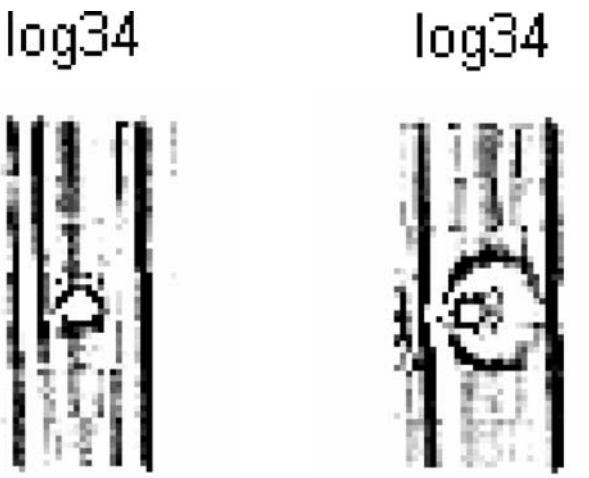

Fig. 4 LOG filtered images of TP-A and TO-I

Conclusions

The results of the experiments confirm our belief that Mueller matrix is sensitive to the shape of the lesion developing in the underlining epithelial layer of the tissue. Precancerous lesions are rigid or semi-rigid mass of transformed cells concentrated in a small area. The refractive index of the lesion is somewhat different because of the changes in the structure of the cell organelles. Transformation also changes the birefringent properties of the lesion.

Thus, the changes in the elasticity, refractive index, and the birefringent properties as well as the irregular shape of the lesion in the precancerous stage help us detect the tumor using polarimetric imaging techniques.

The pseudo-color pictures, contours, and processed images obtained with the samples of intralipid clearly show that the apparatus and analysis techniques are working as intended and support the belief that Mueller matrix images provide a reproducible fingerprint of turbid media. This success opens up the possibility of many further more novel investigations of relevant and interesting areas.

Thus, irregular shapes of the contours together with the features of different Mueller matrix elements can be applied for the diagnosis of malignant tumors in the early stages when they are invisible. Early detection, in turn, will lead to lower mortality rate.

References

1. Roy, R. N. *Textbook of Biophysics*. 1st ed. New Central Book Agency.
2. Cotran, R. S., Kumar, V., Collins, T., & Robbins, S. L. (1999). *Robbins pathologic basis of disease*. 6th ed. (January 15, 1999).
3. Jacques, S. L., Ramella-Roman, J. C., & Lee, K. (2002). Imaging skin pathology with polarized light. *Journal of Biomedical Optics*, *7*(3), 329–340.
4. Demos, S. G., Radousky, H. B., & Alfano, R. R. (2000). Deep subsurface imaging in tissues using spectral and polarization filtering. *Optics Express*, *7*(1), 23.
5. Cameron, B. D., Rakovic, M. J., Kattawar, G. W., Rastegar, S., Wang, L. V., & Cote, G. L. (1998). Measurement and calculation of the two-dimensional backscattering Mueller matrix of a turbid medium. *Optics Letters*, *23*(7), 485.
6. Liu, G. L., Li, Y., & Cameron, B. D. (2002). Polarization-Based Optical Imaging and Processing Techniques with Application to the Cancer Diagnostics. Laser Tissue Interaction XIII, Proceedings of SPIE Vol. 4617
7. Nezhuvingal, A., Li, Y., Anumula, H., & Cameron, B. D. (2003) Mueller Matrix Optical Imaging with Application to Tissue Diagnostics. SPIE USE, V. 3 4961A-24, 22:14:02